Research Paper

Prognostic Impact of Circulating Tumor Cell Detected Using a Novel Fluidic Cell Microarray Chip System in Patients with Breast Cancer

Takeshi Sawada [a,f], Jungo Araki [b], Toshinari Yamashita [c], Manami Masubuchi [b], Tsuneko Chiyoda [b], Mayu Yunokawa [d], Kumiko Hoshi [b], Shoichi Tao [b], Shohei Yamamura [e], Shouki Yatsushiro [e], Kaori Abe [e], Masatoshi Kataoka [e], Tatsu Shimoyama [a], Yoshiharu Maeda [a], Katsumasa Kuroi [c], Kenji Tamura [d], Tsuneo Sawazumi [b], Hironobu Minami [f], Yoshihiko Suda [b], Fumiaki Koizumi [g,*]

[a] Department of Medical Oncology, Tokyo Metropolitan Cancer and Infectious Diseases Center, Komagome Hospital, 3-18-22 Honkomagome, Bunkyo-ku, Tokyo 113-8677, Japan
[b] Konica Minolta, Inc., 1 Sakuramachi, Hino, Tokyo 191-8511, Japan
[c] Department of Breast Surgery, Tokyo Metropolitan Cancer and Infectious Diseases Center, Komagome Hospital, 3-18-22 Honkomagome, Bunkyo-ku, Tokyo 113-8677, Japan
[d] Department of Breast Oncology and Medical Oncology, National Cancer Center Hospital, 5-1-1 Tsukiji, Chuo-ku, Tokyo 104-0045, Japan
[e] Health Research Institute, National Institute of Advanced Industrial Science and Technology (AIST), 2217-14 Hayashi-cho, Takamatsu, Kagawa 761-0395, Japan
[f] Department of Medical Oncology/Hematology, Kobe University Graduate School of Medicine, 7-5-2 Kusunoki-cho, Chuo-ku, Kobe 650-0017, Japan
[g] Division of Clinical Research Support, Tokyo Metropolitan Cancer and Infectious Diseases Center, Komagome Hospital, 3-18-22 Honkomagome, Bunkyo-ku, Tokyo 113-8677, Japan

ABSTRACT

Various types of circulating tumor cell (CTC) detection systems have recently been developed that show a high CTC detection rate. However, it is a big challenge to find a system that can provide better prognostic value than CellSearch in head-to-head comparison. We have developed a novel semi-automated CTC enumeration system (fluidic cell microarray chip system, FCMC) that captures CTC independently of tumor-specific markers or physical properties. Here, we compared the CTC detection sensitivity and the prognostic value of FCMC with CellSearch in breast cancer patients. FCMC was validated in preclinical studies using spike-in samples and in blood samples from 20 healthy donors and 22 breast cancer patients in this study. Using spike-in samples, a statistically higher detection rate ($p = 0.010$) of MDA-MB-231 cells and an equivalent detection rate ($p = 0.497$) of MCF-7 cells were obtained with FCMC in comparison with CellSearch. The number of CTC detected in samples from patients that was above a threshold value as determined from healthy donors was evaluated. The CTC number detected using FCMC was significantly higher than that using CellSearch ($p = 0.00037$). CTC numbers obtained using either FCMC or CellSearch had prognostic value, as assessed by progression free survival. The hazard ratio between CTC+ and CTC− was 4.229 in CellSearch (95% CI, 1.31 to 13.66; $p = 0.01591$); in contrast, it was 11.31 in FCMC (95% CI, 2.245 to 57.0; $p = 0.000244$). CTC detected using FCMC, like the CTC detected using CellSearch, have the potential to be a strong prognostic factor for cancer patients.

© 2016 The Authors. Published by Elsevier B.V. This is an open access article under the CC BY-NC-ND license (http://creativecommons.org/licenses/by-nc-nd/4.0/).

1. Introduction

Circulating tumor cells (CTC) are cancer cells that are present in the blood stream among 5×10^6/mL of leukocytes and 5×10^9/mL of red blood cells (Allard et al., 2004). CTC are considered to be an important clue for estimation of the possibility of metastasis formation (Fidler, 2003) and are expected to be a prognostic marker of cancer patients (Cristofanilli et al., 2005). Therefore numerous technologies for analysis of CTC have been developed in the past decade (Joosse et al., 2014; Haber and Velculescu, 2014; Ignatiadis et al., 2015; Ferreira et al., 2016). One such technology, the CellSearch system, has been used in a number of prospective clinical trials and is the only CTC detection system approved by the FDA. These clinical trials indicated that the number of CTCs detected using CellSearch had prognostic value in patients with breast, colon, prostate, non-small cell lung, small cell lung and gastric cancer (Cristofanilli et al., 2004; Cohen et al., 2008; de Bono et al., 2008; Krebs et al., 2011; Naito et al., 2012; Matsusaka et al., 2010). In patients with breast cancer in particular, CellSearch detection of just one CTC in the early stage had prognostic value (Lucci et al., 2012). Thus, CellSearch is thought of as a firmly established system that can indicate strong prognostic value in breast cancer.

Abbreviations: CTC, circulating tumor cell; FCMC, fluidic cell microarray chip; CM, cell microarray; NCCH, National Cancer Center Hospital; CICK, Tokyo Metropolitan Cancer and Infectious Diseases Center Komagome Hospital; CK, cytokeratin; PFS, progression free survival; PR, partial response; SD, stable disease; PD, disease progression; CT, chemotherapy; HT, hormonotherapy; DGC, density gradient centrifugation; EMT, epithelial mesenchymal-transition.
* Corresponding author.
E-mail address: fkoizumi@cick.jp (F. Koizumi).

However, most of the methods for CTC enumeration, including the CellSearch system, can potentially lose CTCs, which might affect the sensitivity of CTC detection. Because of the low abundance of CTC in blood, almost all methods of CTC detection require enrichment of CTC from blood cells using label-dependent or physical property-based selection (Joosse et al., 2014). These enrichment processes may possibly reduce CTC detection sensitivity. Therefore, an enrichment process with minimal CTC loss that is independent of protein expression or a physical property is needed.

To overcome such problems, we previously developed the cell microarray chip (CM chip) that enables high sensitivity detection of rare cells in blood such as malaria-infected erythrocytes or spiked-in cancer cells (Yatsushiro et al., 2010; Yamamura et al., 2012). The CM chip enables rare cell detection independent of cell surface protein expression with few enrichment steps. In order to increase the detection sensitivity and robustness of the CM chip, we developed a fluidic cell microarray chip (FCMC) device and a semi-automated FCMC system based on the CM chip, which aimed to eliminate the possibilities of target cell loss.

In this article, we show the performance of this FCMC system in preclinical studies and the results of head-to-head comparisons of the CTC detection rate of the FCMC system with that of the CellSearch system in patients with breast cancer. Importantly, we also compare the prognostic impact of the FCMC system with the CellSearch system in this study.

2. Materials and Methods

2.1. Study Participants

All patients and healthy donors in the present studies below provided informed consent and their participation in the studies was approved by the institutional review committee of Konica Minolta, Inc., the National Cancer Center Hospital (NCCH; Tokyo, Japan) and the Tokyo Metropolitan Cancer and Infectious Diseases Center Komagome Hospital (CICK; Tokyo, Japan). Patients who were pathologically diagnosed with breast cancer, and healthy donors who did not have any cancer history were recruited. Patients who had double cancers or who had any prior cancer history were not eligible for the present studies. This work was carried out in accordance with the Code of Ethics of the World Medical Association (Declaration of Helsinki).

2.2. Fluidic Cell-Microarray-Chip Device (FCMC Device)

We developed the FCMC device based on the CM chip as shown in Fig. 1-A. About 18,000 microchambers were contained in the redesigned CM chip; each microchamber was 120 μm in diameter at the top, 90 μm in diameter at the bottom, and 50 μm deep (Fig. 1-B). The proximal and distal distance of microchambers from each other was 200 μm and 300 μm, respectively (Fig. 1-C). We coated BSA on the chip surface on the outside of the microchambers after UV-ozone exposure. A BSA coating prevents nonspecific adsorption of cells onto the surface. This coating supported the movement of untrapped cells into the microchambers. We formed a flow channel by bonding a cover plate to the new CM chip using black double-sided adhesion film. The bonding process formed a flow channel (15 mm wide, 50 mm long and 100 μm deep (Fig. 1-B, D). Each microchamber can hold approximately 50 cells inside as a tight monolayer in a state in which the fluorescent intensity of every cell can be easily analyzed (Fig. 1-E, F). Therefore, one FCMC device can analyze up to 9×10^5 cells. The use of multiple FCMC devices enabled CTC enumeration in this study.

2.3. Blood Processing for the FCMC System

Peripheral blood samples (2 mL, anticoagulated with EDTA) for CTC analysis were collected after withdrawal of the first several milliliters of blood for clinical use to avoid potential skin cell contamination from the venipuncture. Two milliliters of blood sample were processed using Ficoll-Paque PLUS (GE Healthcare, Little Chalfont, UK). Precipitated cells were fixed with 4% formaldehyde, and were then suspended into 340 μL PBS (Supplementary Fig. S1). The workflow of sample processing is shown in Fig. 2-A. Based on preliminary experiments (Supplementary Fig. S2), the samples were processed within three hours after blood collection, and were then analyzed with the FCMC device within three days.

2.4. Formation of Cell Monolayers in Microchambers Using the FCMC Device

The FCMC device was filled with PBS before loading the cell suspension. Cells were trapped in the microchambers as a monolayer by the following steps (Fig. 2-B and Supplementary Fig. S3). One fifth of the cell suspension (68 μL) was loaded from the reservoir tank into the flow channel by suction. The cells had completely settled down on the chip surface within 1 min. At this time, many excess cells remained on the chip surface. We subsequently applied two automated suction methods to improve cell capture efficiency, termed "Suction for Trapping" and "Suction for Monolayer". "Suction for Trapping" involves 10 cycles of a brief suction (suction rate, 0.1 mL/min; total volume of suction, 0.3 μL) and incubation (10 s). This step moves untrapped cells gradually towards downstream microchambers. "Suction for Monolayer" is a long suction (suction rate, 0.1 mL/min; total volume of suction, 41 μL) followed by an incubation (10 s). This step moves overlapped cells out of microchambers. Cells that are present as monolayers at the bottom of the microchambers can maintain their position during the time of "Suction for Monolayer" because the height of the cell monolayer at the bottom of the microchamber (10 μm) means that these cells are little affected by suction flow as the in-silico simulation shows (Fig. 3-A). After ten repetitions of "Suction for Trapping" and "Suction for Monolayer", all cells are completely trapped as a monolayer (Fig. 3-B, C).

2.5. Immunostaining for Discriminating CTCs From Leukocytes

The first immunostaining solution, which included 1:2 diluted anti-cytokeratin (CK) mAb CAM5.2 (Becton, Dickinson and Company, San Jose, CA) and 1:50 diluted anti-human CD45 mAb HI30 (BioLegend, San Diego, CA) in PBS solution containing 1% Tween 20 (Calbiochem, San Diego, CA) and 3% BSA (Thermo Fisher Scientific, Lafayette, CO), was loaded onto the FCMC device. After incubation for 30 min at room temperature and washing with PBS, the second immunostaining solution was then loaded. The second immunostaining solution included 1:500 diluted Alexa Fluor 488 Goat Anti-Mouse IgG1 (γ1) (Life Technologies, Grand Island, NY), 1:500 diluted Alexa Fluor 647 Goat Anti-Mouse IgG2a (γ2a) (Life technologies) and 1:1000 diluted Hoechst 33342 10 mg/mL solution (Life technologies) in PBS solution containing 1% Tween 20 and 3% BSA. After incubation for 30 min at room temperature, unbound mAbs were washed out with PBS.

2.6. Detection of CTCs in Fluorescent Microscopic Images

Immunofluorescent stained cells in the FCMC system were analyzed using an Axio Imager M2 fluorescence microscope equipped with standard filter sets (49, 38HE, 50 for Hoechst 33342, Alexa488, and Alexa 647 respectively), a monochrome CCD camera, (AxioCam MRm), a $5\times$ objective (EC Plan-NEO FLUAR) and ZEN2012 blue edition software (Carl Zeiss, Jena, Germany). Approximately 400 views were captured to cover the entire area of the microchamber. The fluorescence images were analyzed using in-house software that identifies candidate CTCs. First, the software identified cells that were CK$^+$ and Hoechst 33342$^+$. If these cells displayed a strong CD45 signal, the software excluded them as CTC candidates. Next, multiple skilled inspectors examined the list of candidates and manually excluded CD45^{weak} cells from the list of CTC candidates. Each candidate was shown with its

(A)   (B)   (C)

(D)   (E)   (F)
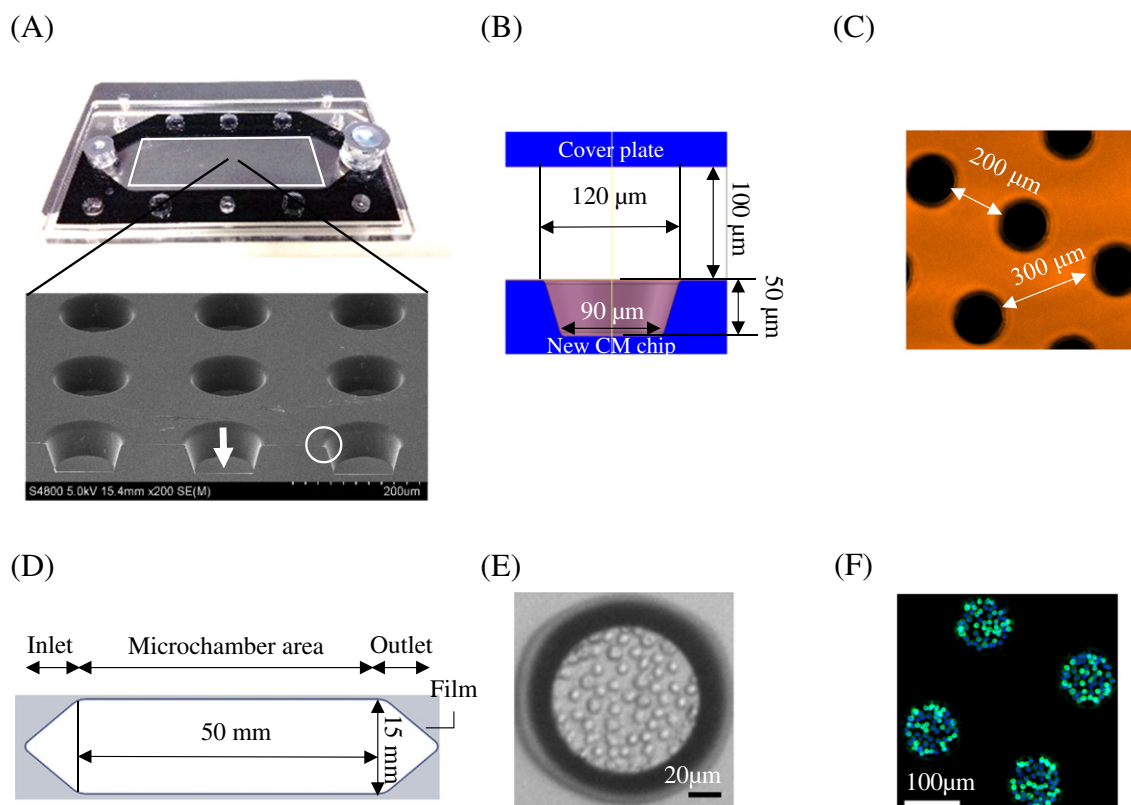

Fig. 1. A schematic outline of CTC detection using the FCMC system. (A) Assembled FCMC device (top side) and cross-sectional scanning electron microscope image of the microchambers (bottom side). The rectangular area indicates the area used for flatness measurement, the arrow indicates the area used for measurement of roughness and the circle enclosing a white line indicates the area used for measurement of the radius of the microchamber rim. (B) A zoomed side view of the flow channel over the microchamber. The depth, and the top and bottom diameter of each microchamber, and the height of the flow channel are indicated. (C) A zoomed top view of the flow channel. Distances between microchambers are indicated. The orange colored area is coated with BSA. (D) A top view of the flow channel. The size of the flow channels and the microchamber area are indicated. (E) Bright field view of cells trapped as a tight monolayer in a microchamber. (F) Immunostained cells in microchambers. All of the cells are trapped in microchambers. Leukocytes are immunostained with an anti-CD45 antibody and labeled with Alexa fluor 488 dye (green). Blue: Hoechst 33342 (nucleus).

microchamber in order to be compared with the intensity of background noise. Bright-field images were also examined for morphological discrimination of non-cell materials.

2.7. Cell Lines

The breast cancer cell lines, MDA-MB-231 and MCF-7, were used for preclinical spike-in experiments. MDA-MB-231 and MCF-7 were obtained from the ATCC (Manassas, VA) and the JCRB Cell Bank (Osaka, Japan), respectively. All cell lines were authenticated by DNA STR profiling. MDA-MB-231 cells were maintained in Leibovitz's L-15 medium (Life technologies), and the MCF-7 cell line was maintained in MEM Earle's medium (Life technologies) containing 10% fetal bovine serum (GE Healthcare), penicillin, streptomycin and amphotericin B (10,000 U/mL, 10 mg/mL and 25 μg/mL, respectively; Sigma-Aldrich, St. Louis, MO) under a humidified atmosphere containing 5% CO_2 at 37 °C.

2.8. Evaluation of the Capture Efficiency of the FCMC System Without Blood Processing

MDA-MB-231 cells, and leukocytes isolated from healthy donor's blood by using Ficoll-Paque PLUS separation medium, were used. Each cell type was fixed with 4% formaldehyde and washed with PBS. MDA-MB231 cells (1×10^3 cells) were spiked into 5×10^5 leukocytes in 68 μL of PBS. MDA-MB231 cells were detected in the cell suspension by the FCMC system without blood processing. Cell capture efficiency was calculated using the detected MDA-MB231 counts divided by the spiked MDA-MB231 counts.

2.9. Evaluation of the FCMC System Using Spiked-in Blood

MDA-MB-231 or MCF-7 cells were spiked into 2 mL of blood for the FCMC system or into 10 mL of blood for the CellSearch system. The spiked cell counts were determined using a serial dilution method. Two milliliters of spiked-in blood was processed using Ficoll-Paque PLUS and two fifths of the volume of the blood were analyzed using two FCMC devices. Ultimately, the detected cell counts per 0.8 mL of blood were obtained (Supplementary Fig. S1). To evaluate linearity of cell recovery, we used 16, 63, 250 or 500 of MDA-MB-231 cell-spiked blood. The slope and coefficient of determination (R^2) were calculated by regression analysis. The percentage recovery of each cell line was calculated using "the detected cell line counts" divided by two fifth of "the spiked cell line counts". The difference in the percentage cell recovery between the FCMC system and the CellSearch system was evaluated using t-test statistical analysis.

2.10. Evaluation of the FCMC System Using Samples From Healthy Donors and Breast Cancer Patients

We analyzed samples from twenty healthy donors and twenty two breast cancer patients using the FCMC system. The healthy donors were recruited in Konica Minolta, Inc. and the patients were recruited in NCCH and CICK. Two milliliters of blood was processed by Ficoll-Paque PLUS and four fifths of the volume of the blood were analyzed by using four FCMC devices. Ultimately, CTC counts per 1.6 mL of blood were obtained (Supplementary Fig. S1). The first five patients in NCCH were analyzed using an FCMC device that has approximately 15,000
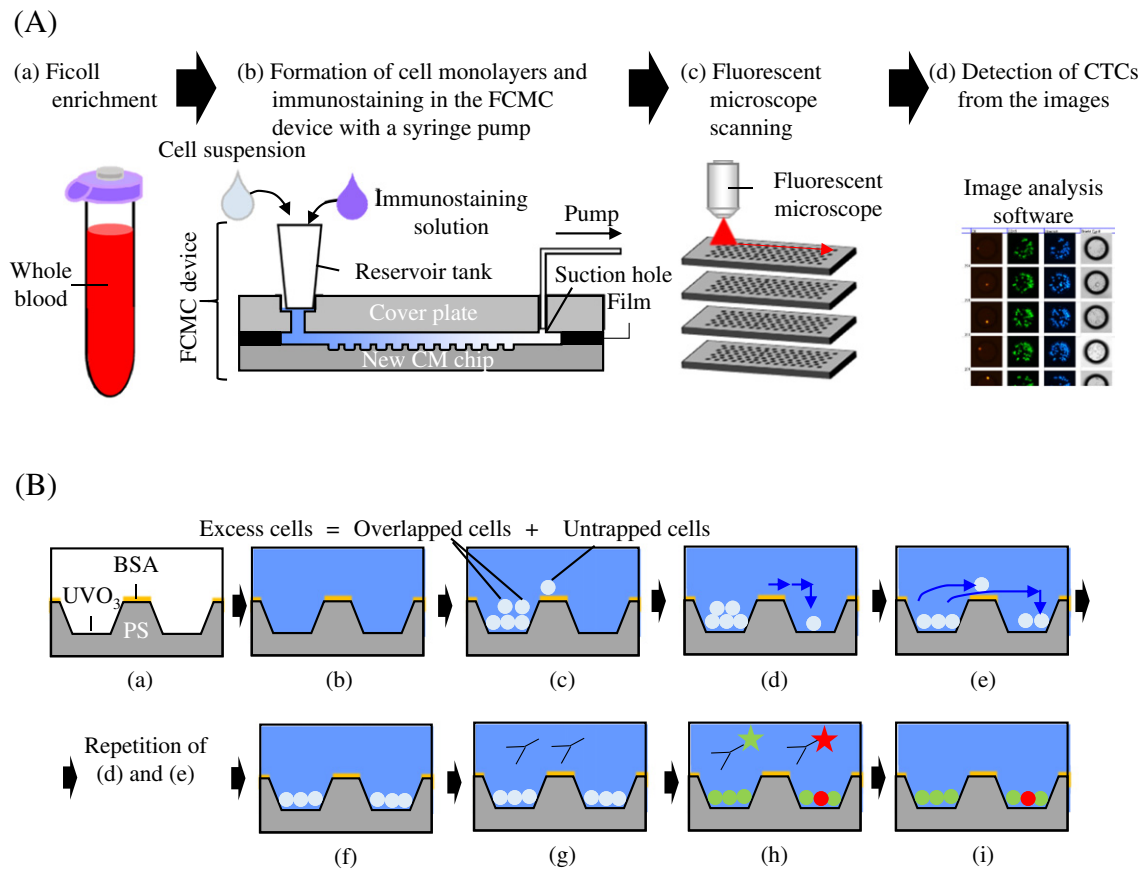
Fig. 2. Workflow of sample processing and movement of cells in the FCMC device. (A) Workflow of sample processing and CTC detection. (a) Blood sample collection and enrichment using Ficoll-Paque PLUS. (b) The cell suspension is loaded into the FCMC device. The cells form monolayers in the microchambers and are immunostained by using a syringe pump. (c) All microchambers are scanned using a fluorescent microscope. (d) CTC are detected from the fluorescent images. (B) Movement of cells in the FCMC device. (a) The new CM chip, which is made from polystyrene (PS), is cleaned with UV ozone and coated with BSA. (b) The FCMC device is washed with PBS. (c) A cell suspension (68 uL) that is equivalent to 0.4 mL of blood is loaded into one FCMC device. (d) After "Suction for Trapping", untrapped cells move into downstream microchambers and settle down on the bottom of these microchambers. The blue arrows indicate flow. (e) After "Suction for Monolayer", overlapped cells are discharged from microchambers and move to the outside of microchambers or to the inside of downstream microchambers. (f) After repetitions of (d) and (e), all cells are trapped in a monolayer. (g), (h), (i) Immunostaining solutions are loaded, incubated and washed.

microchambers in the flow channel. Samples from breast cancer patients were also analyzed using the CellSearch system. We compared CTC counts per 7.5 mL blood of breast cancer patients between the FCMC system and the CellSearch system using Wilcoxon's signed rank test.

2.11. Statistical Analysis Software

EZR (Saitama Medical Center, Jichi Medical University), which is a graphical user interface for R (The R Foundation for Statistical Computing, version 2.13.0), was used for statistical analyses (Kanda, 2013).

3. Results

3.1. Complete Cell Capture From Cultured Cell Suspensions Using the FCMC Device

We developed the FCMC device by mounting a micro fluid channel onto the redesigned CM chip of the previous CM system. An overview of the redesigned system with the micro fluid channel, and its use for CTC detection, is shown in Figs. 1 and 2-A. The new chip has a smooth surface, a flatness area and a sharp edge. The surface roughness (Ra) of the bottom of the microchamber is 9–10 nm (Fig. 1-A, white arrow). The flatness of the microchamber area is 21–25 μm (Fig. 1-A, white rectangle). The edge (R) of the microchamber is lower than 0.005 (Fig. 1-A, white circle). We evaluated the cell-trapping efficiency of the FCMC device using an automated suction algorithm. The suction

algorithm is shown in Supplementary Fig. S3. After initial loading of 6×10^5 leukocytes, only 54% of the leukocytes were trapped in the micro chambers. Untrapped cells were subsequently trapped in the microchambers by repetition of the brief suction and the incubation. Complete cell capture was achieved after a total of ten brief suctions and incubations (Fig. 3-B, C). Cell capture in a monolayer in the microchambers was promoted by the flow in the microfluid channel and by the hydrodynamic design of the flow channel (Fig. 3-A, D). We then evaluated the capture efficiency of 1×10^3 MDA-MB-231 cells mixed with 3×10^5 leukocytes using the FCMC device. After cell capture, we detected MDA-MB 231 by immunofluorescent staining. The percentage detection of the MDA-MB-231 cells was $100 \pm 10\%$ (mean $\pm$ SD). The accuracy of the cell counting chamber used for MDA-MB-231 cell preparation includes 10% of SD. Therefore, the FCMC device had extra-high potential for CTC detection after removal of red blood cells from the blood samples.

3.2. Linearity of the FCMC System Using Spiked-in Blood

The detection efficiency of rare cells in blood using the FCMC system was evaluated using serial dilutions of MDA-MB231 cells spiked into 2 mL of blood from healthy donors. The expected number of spiked-in cells, plotted against the actual number of cells observed in the samples, is shown in Fig. 4-A. Regression analysis of the number of observed tumor cells versus the number of expected tumor cells produced a slope of 0.71, and a coefficient of determination (R^2) of 0.94. The
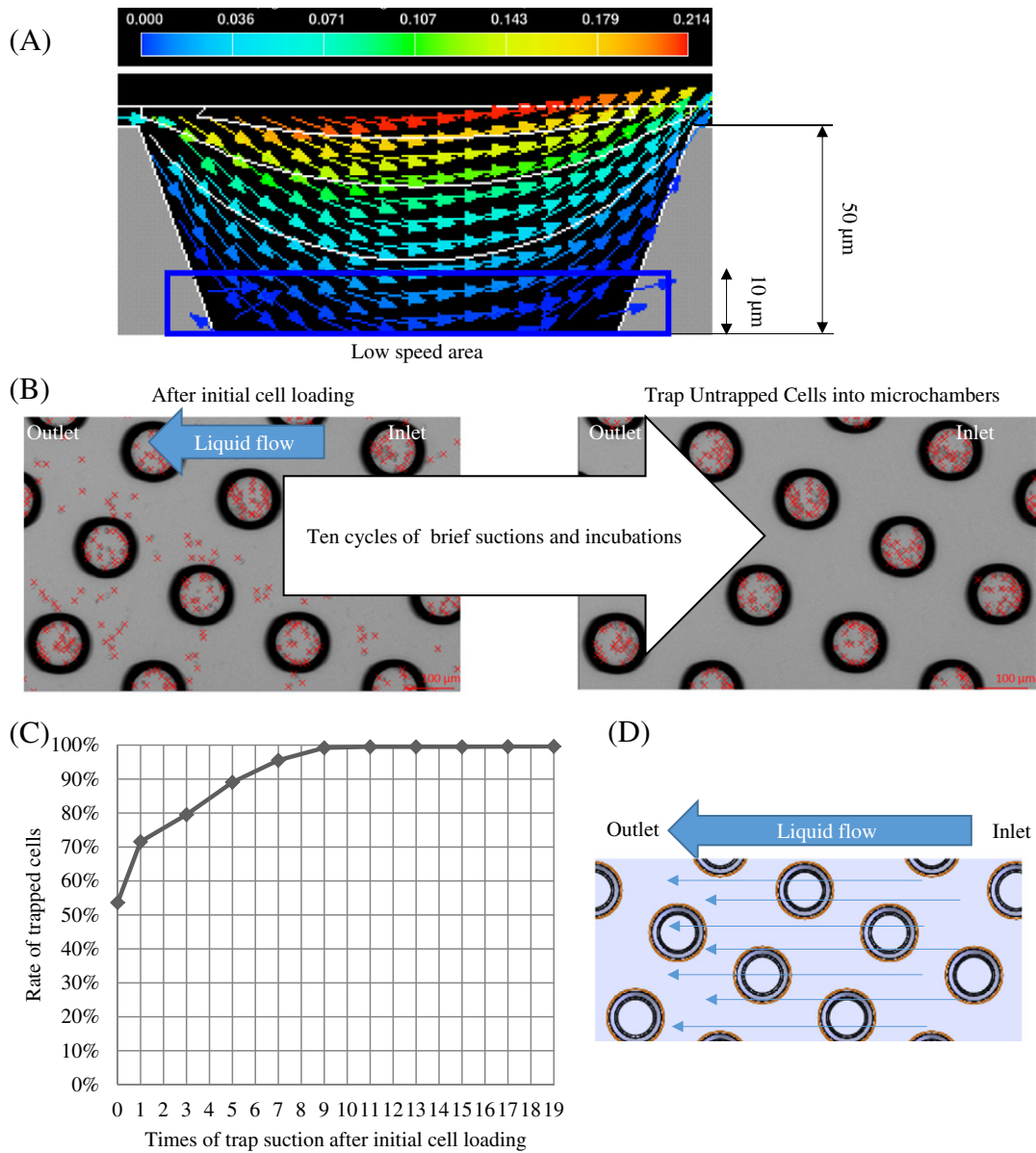
Fig. 3. Excess cells are efficiently and completely trapped into microchambers as monolayers by using the FCMC device with the automated suction algorithm. (A) The flow channel is hydrodynamically designed to capture cells as a monolayer. The flow velocity in the FCMC device was simulated using FLOW-3D software (Flow Science, US), assuming the flow channel of the FCMC device and the flow rate used in this study (0.1 mL/min). Flow is indicated by the arrows. Flow velocity is indicated as a colored image. The unit of flow velocity is $\times 10^{-3}$ cm/min. The cells in the bottom space of the microchamber (area framed in dark blue) receive minimal effects of flow. The depth of the low-speed area is equivalent to the height of a cell monolayer. (B) Left: bright field image of cells in representative microchambers 1 min after incubation of leukocytes loaded into the FCMC device. Right: cells in a microchamber after ten cycles of brief suctions and incubations. The red-colored-crosses indicate leukocytes. (C) Quantification of trapped leukocytes. Leukocytes (6×10^5 cells) were loaded into the FCMC device and incubated for 1 min. After incubation, twenty cycles of brief suction and incubation were applied. Cells trapped in microchambers were counted in each cycle by using a microscope. (D) Microchambers are located so as to trap cells efficiently. The arrows indicate the flow from inlet to outlet. All of the arrows pass over microchambers as shown.

mean percentage of recovered cells was ≥75% ($n = 16$). Individual percentage cell recovery was: 82% ± 42%, 78% ± 26%, 81% ± 19% and 75% ± 14% of 6, 26, 100 and 200 spiked cells, respectively.

3.3. Comparison of the Recovery Rate of Cancer Cells Between the FCMC and the CellSearch System

The spiked cancer cell recovery rate of the FCMC system was compared with that of the CellSearch system using MCF-7 and MDA-MB-231 cell spiked-in blood samples. MCF-7 cells express CK and EpCAM but have low Vimentin expression. MDA-MB-231 cells are CK^{weak}, have low EpCAM expression, and express Vimentin (Supplementary Fig. S4). Each cell line was spiked into blood from a healthy donor so

that the spiked blood was at a concentration of 32 cells per mL. The percentage cell recovery of the two cell lines is shown in Fig. 4-B. Using the FCMC system, the percentage recovery of MDA-MB-231 cells was 66% ± 14%, and that of MCF-7 cells was 73% ± 34%. On the other hand, using the CellSearch system, the percentage recovery of MDA-MB-231 cells was 12% ± 15%, and that of MCF-7 cells was 89% ± 13%. No statistical difference was found between the percentage recovery of MCF-7 cells using the FCMC system and that using the CellSearch system ($p = 0.497$, t-test). In contrast, the percentage recovery of MDA-MB-231 cells obtained using the FCMC system was significantly higher as compared to that obtained using the CellSearch system ($p = 0.010$, t-test). Typical immunofluorescence images of MDA-MB-231 and MCF-7 cells detected using the FCMC system are shown in Fig. 4-C.

(A)

$$y = 0.71x + 1.70$$
$$R^2 = 0.94$$

(B)

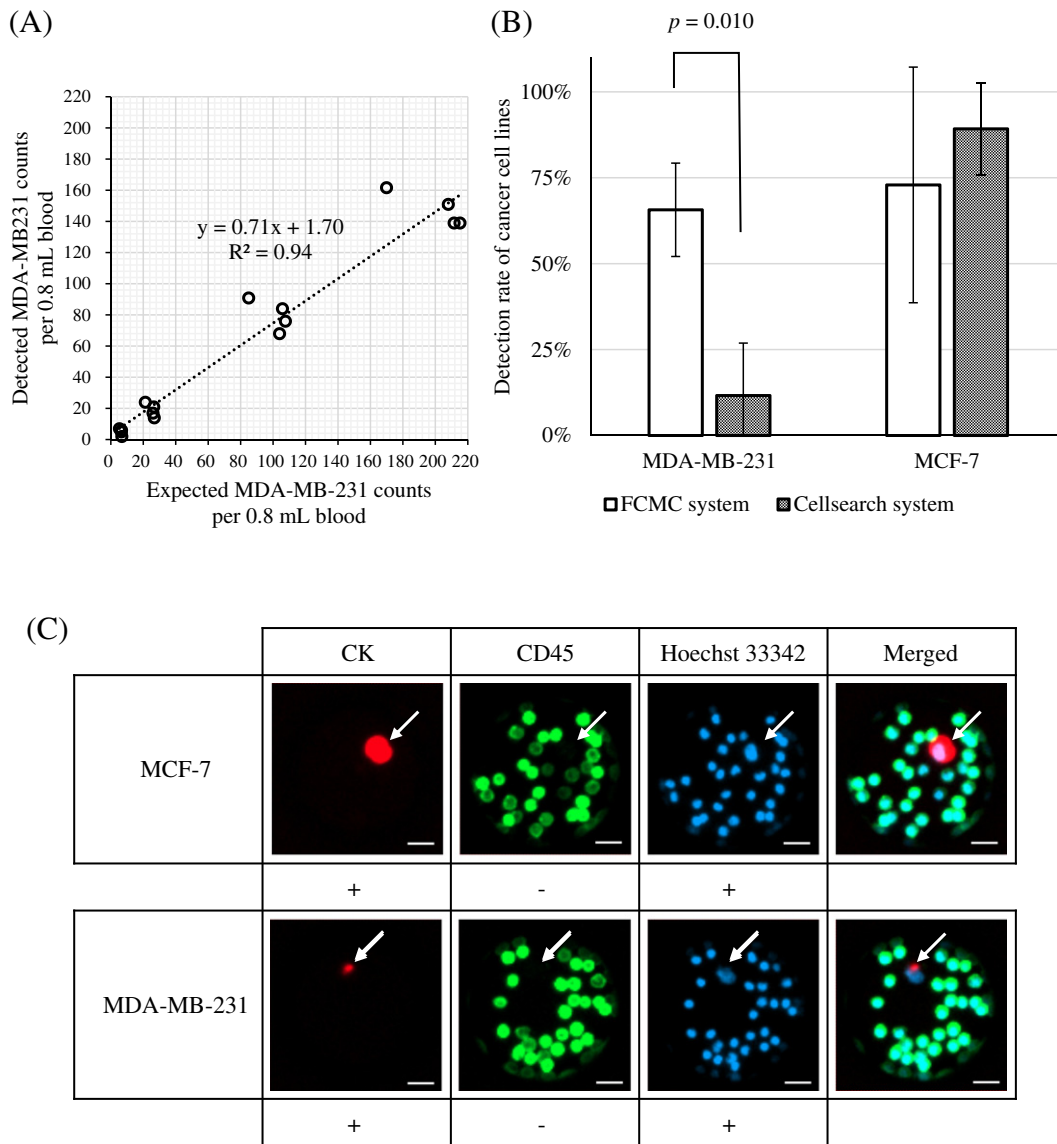$p = 0.010$

□ FCMC system   ▨ Cellsearch system

(C)

Fig. 4. Linearity of cell detection of the FCMC system, and comparison of the spiked cell detection rate of the FCMC and CellSearch systems using spiked-in blood samples. (A) An MDA-MB-231 cell suspension (including approximately 500, 250, 63 or 16 cells) was spiked into 2 mL of blood from healthy donors ($N = 4$). Two-fifth volumes of spiked-in blood were analyzed using two FCMC devices. Shown are the detected MDA-MB-231 cell counts per 0.8 mL blood plotted against the expected MDA-MB-231 counts per 0.8 mL blood (approximately 200, 100, 25 or 6 cells). (B) MDA-MB-231 and MCF-7 breast cancer cell lines were individually spiked into blood from healthy donors so that the spiked cells were at a concentration of 32 cells/mL ($N = 3$). The FCMC system detected a higher percentage of spiked-in MDA-MB-231 cells than the CellSearch system ($p = 0.010$, t-test). There was no statistical difference between the percentage detection of spiked-in MCF-7 cells by the two systems. ($p = 0.497$, t-test.) Error bars represent the SD. Data shown here are representative of three independent experiments for each cell line. (C) Typical images of immunostained cell lines detected by the FCMC system. Red, CK; green, CD45; blue, Hoechst 33342 (nucleus). Scale bar, 20 μm.

3.4. CTC Counts in Samples From Healthy Donors

We also analyzed the CTC count per 1.6 mL of peripheral blood from each of 20 healthy donors in Konica Minolta, Inc. (Tokyo, Japan) using the FCMC system, in order to determine a threshold value for the CTC counts using this system. The number of cells analyzed from 1.6 mL of peripheral blood after enrichment is about 1.6×10^6. The mean ± SD value of these CTC counts was 0.6 ± 0.8, and 90% (18/20) of the samples had CTC counts ≤1 (Table 1). No sample had a CTC count ≥4.

3.5. CTC Counts in Samples From Patients With Advanced Breast Cancer

We then compared the CTC counts detected in samples of patients with advanced breast cancer using the FCMC system with those detected using the CellSearch system (Table 2). Samples from 17 advanced

breast cancer patients from CICK and from 5 advanced breast cancer patients from NCCH were evaluated. All patients were under treatment at the time of blood collection, and then the type of treatment and their responses are noted in Table 2. In total, CTCs were detected in 17/22 (77.3%) of these samples; the FCMC system detected CTCs in all 17 samples whereas, in contrast, the CellSearch system detected CTCs in only 8

Table 1
CTC counts in healthy donors detected using the FCMC system. The CTC counts in 1.6 mL blood of 20 healthy donors were analyzed using the FCMC system.

CTC counts/1.6 mL blood	Number of healthy donors ($N = 20$)	
0	11	(55%)
1	7	(35%)
2	1	(5%)
3	1	(5%)

Table 2

Patient characteristics and the results of CTC counts. The CTC counts of 22 patients with breast cancer were analyzed using the FCMC system or the CellSearch system. *, the CTC counts of patients numbered 1–5 were analyzed using an FCMC device that had about 15,000 microchambers in the flow channel, and the counts of patients numbered 6–22 were analyzed using an FCMC device that had about 18,000 microchambers. **, CTC counts detected in 1.6 mL blood using the FCMC system are normalized to a value of 7.5 mL. All patients were under treatment of chemotherapy or hormonotherapy. The results of the most recent CT evaluation for disease are listed. Abbreviations: female, F. CT, chemotherapy. HT, hormonotherapy. PR, partial response. SD, stable disease. PD, progressive disease.

Patient *	Age/sex	Metastatic site	Treatment type	Current response to therapy	CTC count (FCMC system) /7.5 mL**	CTC count (CellSearch system) /7.5 mL
1	58/F	Lung, bone, liver, adrenal gland, brain	CT	SD	4.7	0
2	64/F	Bone, liver	CT	SD	160	4
3	42/F	Lung, lymph node, brain	CT	PD	52	3
4	63/F	Bone, lymph node, liver, pleura	CT	PD	110	64
5	41/F	Lung, bone, liver	CT	SD	0	0
6	67/F	Bone, liver, lymph node	CT	SD	0	0
7	47/F	Bone, lymph node, brain	CT	SD	160	1
8	54/F	Lung, bone, lymph node, adrenal gland, peritoneum	CT	PR	4.7	0
9	67/F	Liver	HT	SD	9.4	0
10	68/F	Breast, lung, bone	CT	SD	12,400	88
11	52/F	Breast, lung, bone, skin, lymph node, pleura, brain	CT	PD	19	0
12	56/F	Bone, lymph node, adrenal gland	CT	SD	9.4	2
13	53/F	Pleura, brain	CT	SD	4.7	0
14	54/F	Bone	CT	SD	0	0
15	82/F	Pleura, bone	HT	SD	4.7	0
16	67/F	Bone, pleura	HT	SD	0	0
17	82/F	Lung, bone, liver, lymph node	HT	SD	9.4	13
18	47/F	Bone	CT	SD	0	0
19	72/F	Bone	HT	SD	9.4	0
20	77/F	Lymph node	CT	SD	33	0
21	62/F	Lung, bone, liver, lymph node, adrenal gland	HT	SD	230	31
22	41/F	Lung, bone, lymph node	HT	SD	4.7	0

out of these 17 samples. Although the FCMC system detected fewer CTCs than the CellSearch system in one sample (patient number 17), when all of the samples were analyzed the FCMC system detected statistically higher counts of CTCs than those detected by the CellSearch system ($p < 0.00037$, Wilcoxon signed rank test) (Fig. 5-A). There was a good correlation between the counts of CTCs detected with both methods (0.764; Spearman rank-correlation coefficient). Typical immunofluorescent images of a CTC from a patient with breast cancer are shown in Fig. 5-B.

3.6. CTC Counts and Progression Free Survival

We analyzed the association between CTC counts and progression free survival (PFS). PFS was defined as the time between blood sampling for CTC analysis and disease progression (PD). The result of 20 healthy donor samples was used to determine the threshold level of the FCMC system as 3 CTCs/1.6 mL. After a median follow-up period of 206 days, the median PFS was significantly shorter in the patients in whom the number of CTC detected using the FCMC system was above the threshold level (CTC+) (40 days; 95% CI, 0 days to N.E., not estimable) than in the patients in whom the number of detected CTC was not above the threshold level (CTC−) (194 days; 95% CI, 173 days to N.E.; $p = 0.000244$; HR, 11.31; 95% CI, 2.245 to 57.0; $p = 0.003284$) (Fig. 5-C). Similarly, using CellSearch, the median PFS was shorter in the patients in whom the number of detected CTC was above the threshold level of 1/7.5 mL that was determined in a previous study (Allard et al., 2004) (CTC+) (97 days; 95% CI, 0 days to 173 days) than in the patients in whom the number of detected CTC was not above the threshold level (CTC−) (325 days; 95% CI, 33 days to N.E.; $p = 0.0082$; HR, 4.229; 95% CI, 1.31 to 13.66; $p = 0.01591$) (Fig. 5-D). Three patients had been evaluated by CT scanning and had been confirmed as PD at the same time as their blood collection.

4. Discussion

The CellSearch system precedes other methods for CTC detection. Since CellSearch was described various other types of CTC detection systems have been developed and their advantages and disadvantages have been reviewed (Joosse et al., 2014; Haber and Velculescu, 2014; Ignatiadis et al., 2015; Ferreira et al., 2016). Those CTC detection systems are categorized according to the method of CTC enrichment and/or detection. For example, they are based on immunoaffinity (positive selection (Nagrath et al., 2007; Talasaz et al., 2009; Stott et al., 2010; Saucedo-Zeni et al., 2012), negative selection (Liu et al., 2011; Sawada et al., 2016)), biophysical properties (density gradient centrifugation (Campton et al., 2015; Morimoto et al., 2015), microfiltration (Vona et al., 2000; Adams et al., 2014; Sarioglu et al., 2015), inertial force (Ozkumur et al., 2013; Sollier et al., 2014), electrophoresis (Gupta et al., 2012; Peeters et al., 2013), acoustophoresis (Augustsson et al., 2012)), direct imaging (Galanzha and Zharov, 2012; Marrinucci et al., 2012) and functional characteristics (Lu et al., 2010; Alix-Panabieres, 2012). Although the CTC detection rate of some of these methods exceeds that of the CellSearch system, to find a method that shows better clinical significance for the number of detected CTCs compared to CellSearch is considered to be a big challenge. In this study, we showed the high capture efficiency of the FCMC device using cell suspensions, and a good linearity of cell recovery rate using cancer cells spiked into blood. We obtained a higher rate of CTC detection in samples from advanced breast cancer patients using the FCMC system than that using the CellSearch system. Furthermore, we found that the number of CTC detected using the FCMC system provided a better prognostic value than the number detected using the CellSearch system.

We have previously reported the CM chip that enables precise estimation of rare cell counts in blood including spiked-in cultured cancer cells (Yatsushiro et al., 2010; Yamamura et al., 2012). Although the CM chip produced excellent results in a preclinical study, we considered that precise enumeration of CTCs requires analysis of all cells, including the excess cells that might be excluded from the chambers. Thus it was considered that washing of the chip surface might result in the loss of such cells, and may lead to an underestimation of the CTCs present in the sample. Excess cells were classified as "untrapped cells" and "overlapped cells" (Fig. 2-B). Untrapped cells are cells that remain outside of the microchambers. Overlapped cells are cells that are inside of the microchambers but have not adhered to the bottom of the
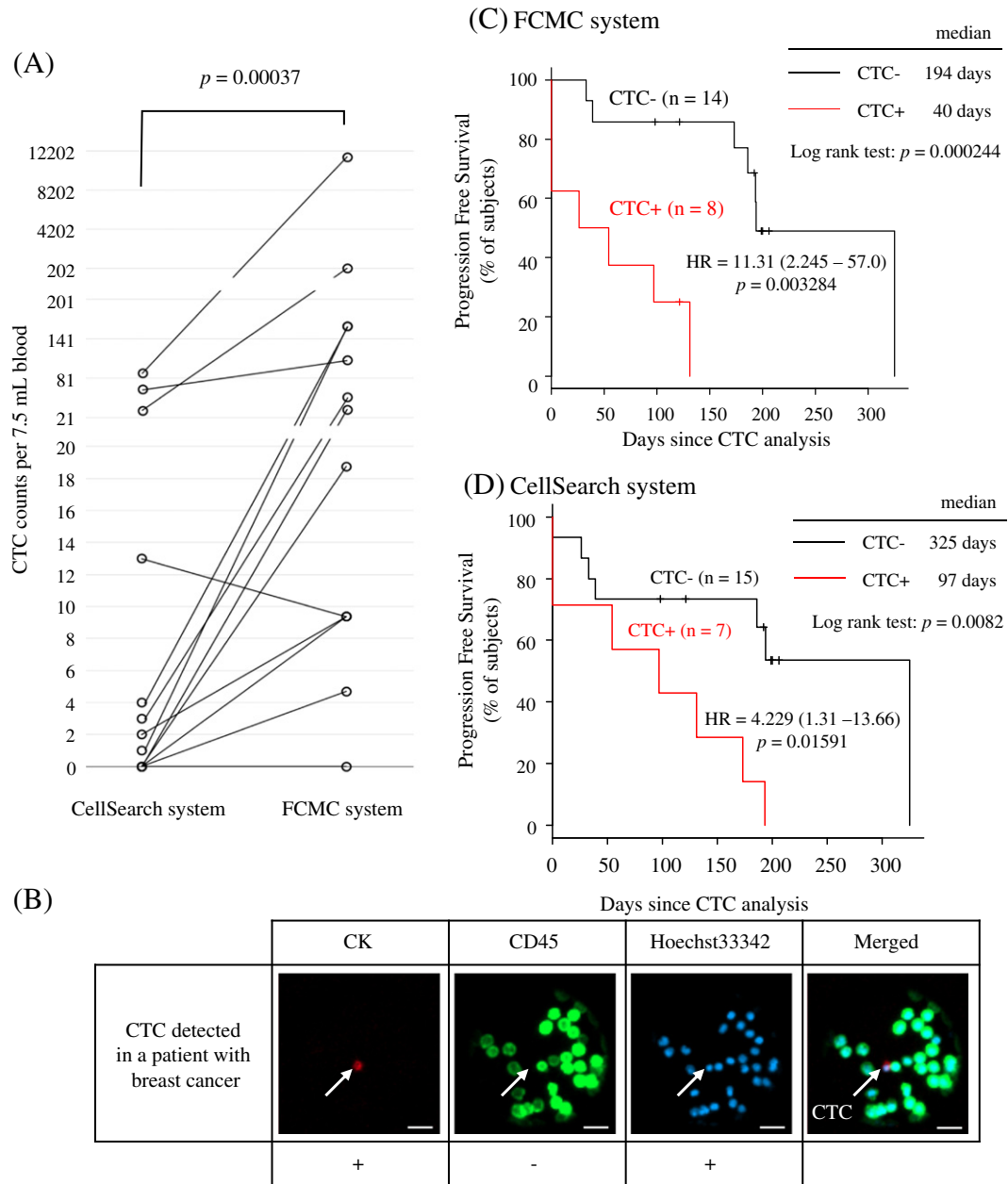
Fig. 5. Comparison of the CTC counts detected in patients with breast cancer using the FCMC system and the CellSearch system, and progression free survival in patients in whom CTC were detected or not detected using the FCMC system or the CellSearch system. (A) The CTC counts of twenty-two patients with breast cancer were evaluated. For comparison with the CellSearch system, the results of the FCMC system from 1.6 mL blood were normalized to a value of 7.5 mL. The number of CTC counts detected using the FCMC system was statistically higher than that using the CellSearch system ($p = 0.00037$, Wilcoxon signed rank test). (B) Typical immunofluorescence stained CTC images of a patient with breast cancer. CTC was defined as cytokeratin (CK) positive, CD45 negative and Hoechst 33342 (nucleus) positive. Scale bar, 20 μm. (C,D) Kaplan-Meier curves of progression free survival (PFS) in patients in whom CTC were detected (CTC+) or not detected (CTC−) using (C) the FCMC system or (D) the CellSearch system are shown. CTC+ is defined as detected CTC counts that are above the threshold level of each system (FCMC, 3 CTC/1.6 mL; CellSearch, 1 CTC/7.5 mL). The log-rank test of PFS showed significant differences according to CTC detection in both systems (FCMC: $p = 0.000244$, CellSearch: $p = 0.0082$). The median PFS of CTC+ patients (40 days; 95% CI, 0 to N.E., not estimable) and CTC− patients (194 days; 95% CI, 173 to N.E.) as assessed using the FCMC system is shown in (C). The median PFS of CTC+ patients (97 days; 95% CI, 0 to 173) and CTC− patients (325 days; 95% CI, 33 to N.E.) as assessed using the CellSearch system is shown in (D). The hazard ratio for PFS was 11.31 (95% confidence interval [CI], 2.245 to 57.0; $p = 0.003284$) for CTC+ patients as compared with CTC− patients using the FCMC system, and was 4.229 (95% CI, 1.31 to 13.66; $p = 0.01591$) for CTC+ patients as compared with CTC− patients using the CellSearch system. Patients remained in the study unless they met a criterion for disease progression.

microchamber as a cell monolayer. In order to trap all of the cells as a monolayer in the microchambers, we improved the CM chip and adopted an automated suction algorithm (Supplementary Fig. S3) which enables efficient cell trapping as a monolayer. We arranged the positions of the microchambers between the inlet and the outlet in order to trap cells efficiently during suction (Fig. 3-D). In an in silico flow simulation, the FCMC device has a low-speed area in a microchamber at a height of 10 μm from the bottom, and this helps to retain cells as a monolayer (Fig. 3-A). Cells can be trapped as a

monolayer in all of the microchambers only by use of the FCMC device with this automated suction algorithm.

In this study, the FCMC system showed higher sensitivity in detection of CTCs in patients with advanced breast cancer than CellSearch. A previous report showed the presence of CTC that were CK+ and EpCAM− in the blood that was discarded by CellSearch after EpCAM-based enrichment (Wit et al., 2015). The FCMC system has the advantage that it enriches CTC independent of CTC EpCAM expression, which enables detection of such CK+ and EpCAM− CTC. Additionally,

the FCMC system adopts only a density gradient centrifugation (DGC)-based enrichment step. DGC-based CTC enrichment is often combined with another enrichment procedure such as depletion of CD45$^+$ cells because it is difficult to detect CTC in the presence of too many residual leukocytes (Lustberg et al., 2012). Although the loss of cells is kept to a minimum in DGC-based enrichment, additional enrichment steps may induce unexpected target cell loss. In the FCMC system, one FCMC device can completely capture about 9×10^5 cells. Generally, the mean recovery numbers of cells by the DGC-based enrichment step is 1.0×10^6 cells/mL of blood (Nilsson et al., 2008); therefore, several FCMC devices are sufficient for enumeration of CTC in that situation. This efficiency may contribute to the high sensitivity in CTC detection of the FCMC system. However, the CTC positive detection rate is still low at 36.4% (8/22), even in the FCMC system. The probable reason is that all patients in this study were under treatment, which might be expected to result in low CTC counts as suggested in previous reports (Riethdorf et al., 2010; Pierga et al., 2008). In order to increase the CTC detection rate, it might be helpful to use arterial blood instead of peripheral blood (Terai et al., 2015).

In spike-in experiments, the FCMC system could detect EpCAM$^-$, CK^{weak} and Vimentin$^+$ MDA-MB-231 cells (Fig. 4-C, Supplementary Fig. S4). The presence of CTCs that express mesenchymal components such as vimentin, the so called Epithelial Mesenchymal-Transition (EMT)-CTC, was previously reported in advanced breast cancer patients, and the expression level of such components changes dramatically in disease progression (Yu et al., 2013). Moreover, recent reports have shown that the heterogeneity of CTC reflects various degrees of epithelial and mesenchymal cell-surface expression depending on the EMT status of the CTC (Polioudaki et al., 2015; Satelli et al., 2015). Indeed, variation in the level of CK expression was observed in the CTC detected in this study (Supplementary Fig. S5). Although proof of the expression of mesenchymal components in CTC is lacking in this study, detection of those cells using the FCMC system may also contribute to the high sensitivity in CTC detection of this system. The FCMC system includes precise location information regarding the chamber that includes the target cell. It therefore enables recovery of target cells for further analysis. Future molecular characterization of those CTCs may reveal the relationship between disease progression and various types of CTCs.

Regarding the prognostic value of CTC, detection of CTCs over the threshold value (CTC + patients) in both the FCMC and CellSearch system was a worse prognostic factor in this study. The significant point that needs to be noted here is that the hazard ratio between CTC + and CTC − patients using the FCMC system was much greater than that between CTC + and CTC − patients using CellSearch. This result indicated that, like the CTC detected using CellSearch, the number of CTC detected using the FCMC system also has the potential to be a strong prognostic marker for cancer patients. An important question is why the FCMC system results have a better prognostic value than the CellSearch results in this study. One possible reason is that the FCMC system detected EMT-CTC. It has been suggested that the presence of EMT-CTC may be associated with an unfavorable outcome (Joosse et al., 2012). EMT is assumed to be an essential state for metastasis (Gunasinghe et al., 2012), and therefore a relationship between the detection of EMT-CTC and short time to disease progression is reasonable. On the other hand, in contradiction to our result, a previous report showed that the presence of EpCAM$^-$ and CK$^+$ CTC was related to a favorable outcome (Wit et al., 2015). Additionally, we could not find a relationship between the number of metastatic sites and the CTC counts using the FCMC system. Both our study and the previous study analyzed a small number of patients, which makes it difficult to come to any definitive conclusion.

Recently, the presence of the aggregates containing two or more CTCs (CTC clusters) has also been associated with poor prognosis in patients with metastatic cancer (Aceto et al., 2014). In addition, CTC clusters are considered as biomarkers for early detection of cancer (Carlsson et al., 2014) and as a potential tool for the monitoring of tumor-immune

cell interactions (Sarioglu et al., 2015). The FCMC system is capable of detecting CTC clusters in a spike-in experiment using MCF-7 cells (Supplementary Fig. S6), however, we did not detect any CTC clusters in this patient study. We consider that the limited number of patients and healthy volunteers is a limitation of this study. We also consider that the use of PFS as an indicator for evaluating and estimating the clinical significance of CTC counts is not sufficient. In order to confirm the findings in this study, a larger study is required with evaluation of overall survival of the patients.

In Memoriam Statement

In memoriam of Tsuneko Chiyoda, a fountainhead of knowledge and an eternal example of complete dedication. She has left behind a rich harvest of memories to cherish, honor and emulate.

Acknowledgements

Appendix A. Supplementary Data

Supplementary data to this article can be found online at http://dx. doi.org/10.1016/j.ebiom.2016.07.027.

References

Aceto, N., Bardia, A., Miyamoto, D.T., Donaldson, M.C., Wittner, B.S., Spencer, J.A., Yu, M., Pely, A., Engstrom, A., Zhu, H., Brannigan, B.W., Kapur, R., Stott, S.L., Shioda, T., Ramaswamy, S., Ting, D.T., Lin, C.P., Toner, M., Haber, D.A., Maheswaran, S., 2014. Circulating tumor cell clusters are oligoclonal precursors of breast cancer metastasis. Cell 158, 1110–1122.

Adams, D.L., Zhu, P., Makarova, O.V., Martin, S.S., Charpentier, M., Chumsri, S., Li, S., Amstutz, P., Tang, C.M., 2014. The systematic study of circulating tumor cell isolation using lithographic microfilters. RSC Adv. 9, 4334–4342.

Alix-Panabieres, C., 2012. EPISPOT assay: detection of viable DTCs/CTCs in solid tumor patients. Recent Results Cancer Res. 195, 69–76.

Allard, W.J., Matera, J., Miller, M.C., Repollet, M., Connelly, M.C., Rao, C., Tibbe, A.G., Uhr, J.W., Terstappen, L.W., 2004. Tumor cells circulate in the peripheral blood of all major carcinomas but not in healthy subjects or patients with nonmalignant diseases. Clin. Cancer Res. 10, 6897–6904.

Augustsson, P., Magnusson, C., Nordin, M., Lilja, H., Laurell, T., 2012. Microfluidic, label-free enrichment of prostate cancer cells in blood based on acoustophoresis. Anal. Chem. 84, 7954–7962.

Campton, D.E., Ramirez, A.B., Nordberg, J.J., Drovetto, N., Clein, A.C., Varshavskaya, P., Friemel, B.H., Quarre, S., Breman, A., Dorschner, M., Blau, S., Blau, C.A., Sabath, D.E., Stilwell, J.L., Kaldjian, E.P., 2015. High-recovery visual identification and single-cell retrieval of circulating tumor cells for genomic analysis using a dual-technology platform integrated with automated immunofluorescence staining. BMC Cancer 15, 360.

Carlsson, A., Nair, V.S., Luttgen, M.S., Keu, K.V., Horng, G., Vasanawala, M., Kolatkar, A., Jamali, M., Iagaru, A.H., Kuschner, W., Loo Jr., B.W., Shrager, J.B., Bethel, K., Hoh, C.K., Bazhenova, L., Nieva, J., Kuhn, P., Gambhir, S.S., 2014. Circulating tumor microemboli diagnostics for patients with non-small-cell lung cancer. J. Thorac. Oncol. 9, 1111–1119.

Cohen, S.J., Punt, C.J., Iannotti, N., Saidman, B.H., Sabbath, K.D., Gabrail, N.Y., Picus, J., Morse, M., Mitchell, E., Miller, M.C., Doyle, G.V., Tissing, H., Terstappen, L.W., Meropol, N.J., 2008. Relationship of circulating tumor cells to tumor response, progression-free survival, and overall survival in patients with metastatic colorectal cancer. J. Clin. Oncol. 26, 3213–3221.

Cristofanilli, M., Budd, G.T., Ellis, M.J., Stopeck, A., Matera, J., Miller, M.C., Reuben, J.M., Doyle, G.V., Allard, W.J., Terstappen, L.W., Hayes, D.F., 2004. Circulating tumor cells, disease progression, and survival in metastatic breast cancer. N. Engl. J. Med. 351, 781–791.

Cristofanilli, M., Hayes, D.F., Budd, G.T., Ellis, M.J., Stopeck, A., Reuben, J.M., Doyle, G.V., Matera, J., Allard, W.J., Miller, M.C., Fritsche, H.A., Hortobagyi, G.N., Terstappen, L.W., 2005. Circulating tumor cells: a novel prognostic factor for newly diagnosed metastatic breast cancer. J. Clin. Oncol. 23, 1420–1430.

de Bono, J.S., Scher, H.I., Montgomery, R.B., Parker, C., Miller, M.C., Tissing, H., Doyle, G.V., Terstappen, L.W., Pienta, K.J., Raghavan, D., 2008. Circulating tumor cells predict survival benefit from treatment in metastatic castration-resistant prostate cancer. Clin. Cancer Res. 14, 6302–6309.

Ferreira, M.M., Ramani, V.C., Jeffrey, S.S., 2016. Circulating tumor cell technologies. Mol. Oncol. 10, 374–394.

Fidler, I.J., 2003. The pathogenesis of cancer metastasis: the 'seed and soil' hypothesis revisited. Nat. Rev. Cancer 3, 453–458.

Galanzha, E.I., Zharov, V.P., 2012. Photoacoustic flow cytometry. Methods 57, 280–296.

Gunasinghe, N.P., Wells, A., Thompson, E.W., Hugo, H.J., 2012. Mesenchymal-epithelial transition (MET) as a mechanism for metastatic colonisation in breast cancer. Cancer Metastasis Rev. 31, 469–478.

Gupta, V., Jafferji, I., Garza, M., Melnikova, V.O., Hasegawa, D.K., Pethig, R., Davis, D.W., 2012. ApoStream(), a new dielectrophoretic device for antibody independent isolation and recovery of viable cancer cells from blood. Biomicrofluidics 6, 24133.

Haber, D.A., Velculescu, V.E., 2014. Blood-based analyses of cancer: circulating tumor cells and circulating tumor DNA. Cancer Discov. 4, 650–661.

Ignatiadis, M., Lee, M., Jeffrey, S.S., 2015. Circulating tumor cells and circulating tumor DNA: challenges and opportunities on the path to clinical utility. Clin. Cancer Res. 21, 4786–4800.

Joosse, S.A., Hannemann, J., Spotter, J., Bauche, A., Andreas, A., Muller, V., Pantel, K., 2012. Changes in keratin expression during metastatic progression of breast cancer: impact on the detection of circulating tumor cells. Clin. Cancer Res. 18, 993–1003.

Joosse, S.A., Gorges, T.M., Pantel, K., 2014. Biology, detection, and clinical implications of circulating tumor cells. EMBO Mol. Med. 7, 1–11.

Kanda, Y., 2013. Investigation of the freely available easy-to-use software 'EZR' for medical statistics. Bone Marrow Transplant. 48, 452–458.

Krebs, M.G., Sloane, R., Priest, L., Lancashire, L., Hou, J.M., Greystoke, A., Ward, T.H., Ferraldeschi, R., Hughes, A., Clack, G., Ranson, M., Dive, C., Blackhall, F.H., 2011. Evaluation and prognostic significance of circulating tumor cells in patients with non-small-cell lung cancer. J. Clin. Oncol. 29, 1556–1563.

Liu, Z., Fusi, A., Klopocki, E., Schmittel, A., Tinhofer, I., Nonnenmacher, A., Keilholz, U., 2011. Negative enrichment by immunomagnetic nanobeads for unbiased characterization of circulating tumor cells from peripheral blood of cancer patients. J. Transl. Med. 9, 70.

Lu, J., Fan, T., Zhao, Q., Zeng, W., Zaslavsky, E., Chen, J.J., Frohman, M.A., Golightly, M.G., Madajewicz, S., Chen, W.T., 2010. Isolation of circulating epithelial and tumor progenitor cells with an invasive phenotype from breast cancer patients. Int. J. Cancer 126, 669–683.

Lucci, A., Hall, C.S., Lodhi, A.K., Bhattacharyya, A., Anderson, A.E., Xiao, L., Bedrosian, I., Kuerer, H.M., Krishnamurthy, S., 2012. Circulating tumour cells in non-metastatic breast cancer: a prospective study. Lancet Oncol. 13, 688–695.

Lustberg, M., Jatana, K.R., Zborowski, M., Chalmers, J.J., 2012. Emerging technologies for CTC detection based on depletion of normal cells. Recent Results Cancer Res. 195, 97–110.

Marrinucci, D., Bethel, K., Kolatkar, A., Luttgen, M.S., Malchiodi, M., Baehring, F., Voigt, K., Lazar, D., Nieva, J., Bazhenova, L., Ko, A.H., Korn, W.M., Schram, E., Coward, M., Yang, X., Metzner, T., Lamy, R., Honnatti, M., Yoshioka, C., Kunken, J., Petrova, Y., Sok, D., Nelson, D., Kuhn, P., 2012. Fluid biopsy in patients with metastatic prostate, pancreatic and breast cancers. Phys. Biol. 9, 016003.

Matsusaka, S., Chin, K., Ogura, M., Suenaga, M., Shinozaki, E., Mishima, Y., Terui, Y., Mizunuma, N., Hatake, K., 2010. Circulating tumor cells as a surrogate marker for determining response to chemotherapy in patients with advanced gastric cancer. Cancer Sci. 101, 1067–1071.

Morimoto, A., Mogami, T., Watanabe, M., Iijima, K., Akiyama, Y., Katayama, K., Futami, T., Yamamoto, N., Sawada, T., Koizumi, F., Koh, Y., 2015. High-density dielectrophoretic microwell array for detection, capture, and single-cell analysis of rare tumor cells in peripheral blood. PLoS One 10, e0130418.

Nagrath, S., Sequist, L.V., Maheswaran, S., Bell, D.W., Irimia, D., Ulkus, L., Smith, M.R., Kwak, E.L., Digumarthy, S., Muzikansky, A., Ryan, P., Balis, U.J., Tompkins, R.G., Haber, D.A., Toner, M., 2007. Isolation of rare circulating tumour cells in cancer patients by microchip technology. Nature 450, 1235–1239.

Naito, T., Tanaka, F., Ono, A., Yoneda, K., Takahashi, T., Murakami, H., Nakamura, Y., Tsuya, A., Kenmotsu, H., Shukuya, T., Kaira, K., Koh, Y., Endo, M., Hasegawa, S., Yamamoto, N., 2012. Prognostic impact of circulating tumor cells in patients with small cell lung cancer. J. Thorac. Oncol. 7, 512–519.

Nilsson, C., Aboud, S., Karlen, K., Hejdeman, B., Urassa, W., Biberfeld, G., 2008. Optimal blood mononuclear cell isolation procedures for gamma interferon enzyme-linked immunospot testing of healthy Swedish and Tanzanian subjects. Clin. Vaccine Immunol. 15, 585–589.

Ozkumur, E., Shah, A.M., Ciciliano, J.C., Emmink, B.L., Miyamoto, D.T., Brachtel, E., Yu, M., Chen, P.I., Morgan, B., Trautwein, J., Kimura, A., Sengupta, S., Stott, S.L., Karabacak, N.M., Barber, T.A., Walsh, J.R., Smith, K., Spuhler, P.S., Sullivan, J.P., Lee, R.J., Ting, D.T., Luo, X., Shaw, A.T., Bardia, A., Sequist, L.V., Louis, D.N., Maheswaran, S., Kapur, R., Haber, D.A., Toner, M., 2013. Inertial focusing for tumor antigen-dependent and -independent sorting of rare circulating tumor cells. Sci. Transl. Med. 5, 179ra47.

Peeters, D.J., De Laere, B., Van den Eynden, G.G., Van Laere, S.J., Rothe, F., Ignatiadis, M., Sieuwerts, A.M., Lambrechts, D., Rutten, A., van Dam, P.A., Pauwels, P., Peeters, M., Vermeulen, P.B., Dirix, L.Y., 2013. Semiautomated isolation and molecular characterisation of single or highly purified tumour cells from CellSearch enriched blood samples using dielectrophoretic cell sorting. Br. J. Cancer 108, 1358–1367.

Pierga, J.Y., Bidard, F.C., Mathiot, C., Brain, E., Delaloge, S., Giachetti, S., de Cremoux, P., Salmon, R., Vincent-Salomon, A., Marty, M., 2008. Circulating tumor cell detection predicts early metastatic relapse after neoadjuvant chemotherapy in large operable and locally advanced breast cancer in a phase II randomized trial. Clin. Cancer Res. 14, 7004–7010.

Polioudaki, H., Agelaki, S., Chiotaki, R., Politaki, E., Mavroudis, D., Matikas, A., Georgoulias, V., Theodoropoulos, P.A., 2015. Variable expression levels of keratin and vimentin reveal differential EMT status of circulating tumor cells and correlation with clinical characteristics and outcome of patients with metastatic breast cancer. BMC Cancer 15, 399.

Riethdorf, S., Muller, V., Zhang, L., Rau, T., Loibl, S., Komor, M., Roller, M., Huober, J., Fehm, T., Schrader, I., Hilfrich, J., Holms, F., Tesch, H., Eidtmann, H., Untch, M., von Minckwitz, G., Pantel, K., 2010. Detection and HER2 expression of circulating tumor cells: prospective monitoring in breast cancer patients treated in the neoadjuvant GeparQuattro trial. Clin. Cancer Res. 16, 2634–2645.

Sarioglu, A.F., Aceto, N., Kojic, N., Donaldson, M.C., Zeinali, M., Hamza, B., Engstrom, A., Zhu, H., Sundaresan, T.K., Miyamoto, D.T., Luo, X., Bardia, A., Wittner, B.S., Ramaswamy, S., Shioda, T., Ting, D.T., Stott, S.L., Kapur, R., Maheswaran, S., Haber, D.A., Toner, M., 2015. A microfluidic device for label-free, physical capture of circulating tumor cell clusters. Nat. Methods 12, 685–691.

Satelli, A., Mitra, A., Brownlee, Z., Xia, X., Bellister, S., Overman, M.J., Kopetz, S., Ellis, L.M., Meng, Q.H., Li, S., 2015. Epithelial-mesenchymal transitioned circulating tumor cells capture for detecting tumor progression. Clin. Cancer Res. 21, 899–906.

Saucedo-Zeni, N., Mewes, S., Niestroj, R., Gasiorowski, L., Murawa, D., Nowaczyk, P., Tomasi, T., Weber, E., Dworacki, G., Morgenthaler, N.G., Jansen, H., Propping, C., Sterzynska, K., Dyszkiewicz, W., Zabel, M., Kiechle, M., Reuning, U., Schmitt, M., Lucke, K., 2012. A novel method for the in vivo isolation of circulating tumor cells from peripheral blood of cancer patients using a functionalized and structured medical wire. Int. J. Oncol. 41, 1241–1250.

Sawada, T., Watanabe, M., Fujimura, Y., Yagishita, S., Shimoyama, T., Maeda, Y., Kanda, S., Yunokawa, M., Tamura, K., Tamura, T., Minami, H., Koh, Y., Koizumi, F., 2016. Sensitive cytometry based system for enumeration, capture and analysis of gene mutations of circulating tumor cells. Cancer Sci. 107, 307–314.

Sollier, E., Go, D.E., Che, J., Gossett, D.R., O'Byrne, S., Weaver, W.M., Kummer, N., Rettig, M., Goldman, J., Nickols, N., McCloskey, S., Kulkarni, R.P., Di Carlo, D., 2014. Size-selective collection of circulating tumor cells using Vortex technology. Lab Chip 14, 63–77.

Stott, S.L., Hsu, C.H., Tsukrov, D.I., Yu, M., Miyamoto, D.T., Waltman, B.A., Rothenberg, S.M., Shah, A.M., Smas, M.E., Korir, G.K., Floyd Jr., F.P., Gilman, A.J., Lord, J.B., Winokur, D., Springer, S., Irimia, D., Nagrath, S., Sequist, L.V., Lee, R.J., Isselbacher, K.J., Maheswaran, S., Haber, D.A., Toner, M., 2010. Isolation of circulating tumor cells using a microvortex-generating herringbone-chip. Proc. Natl. Acad. Sci. U. S. A. 107, 18392–18397.

Talasaz, A.H., Powell, A.A., Huber, D.E., Berbee, J.G., Roh, K.H., Yu, W., Xiao, W., Davis, M.M., Pease, R.F., Mindrinos, M.N., Jeffrey, S.S., Davis, R.W., 2009. Isolating highly enriched populations of circulating epithelial and other rare cells from blood using a magnetic sweeper device. Proc. Natl. Acad. Sci. U. S. A. 106, 3970–3975.

Terai, M., Mu, Z., Eschelman, D.J., Gonsalves, C.F., Kageyama, K., Chervoneva, I., Orloff, M., Weight, R., Mastrangelo, M.J., Cristofanilli, M., Sato, T., 2015. Arterial blood, rather than venous blood, is a better source for circulating melanoma cells. EBioMedicine 2, 1821–1826.

Vona, G., Sabile, A., Louha, M., Sitruk, V., Romana, S., Schutze, K., Capron, F., Franco, D., Pazzagli, M., Vekemans, M., Lacour, B., Brechot, C., Paterlini-Brechot, P., 2000. Isolation by size of epithelial tumor cells: a new method for the immunomorphological and molecular characterization of circulatingtumor cells. Am. J. Pathol. 156, 57–63.

Wit, S., Dalum, G., Lenferink, A.T., Tibbe, A.G., Hiltermann, T.J., Groen, H.J., van Rijn, C.J., Terstappen, L.W., 2015. The detection of EpCAM(+) and EpCAM(−) circulating tumor cells. Sci. Rep. 5, 12270.

Yamamura, S., Yatsushiro, S., Yamaguchi, Y., Abe, K., Shinohara, Y., Tamiya, E., Baba, Y., Kataoka, M., 2012. Accurate detection of carcinoma cells by use of a cell microarray chip. PLoS One 7, e32370.

Yatsushiro, S., Yamamura, S., Yamaguchi, Y., Shinohara, Y., Tamiya, E., Horii, T., Baba, Y., Kataoka, M., 2010. Rapid and highly sensitive detection of malaria-infected erythrocytes using a cell microarray chip. PLoS One 5, e13179.

Yu, M., Bardia, A., Wittner, B.S., Stott, S.L., Smas, M.E., Ting, D.T., Isakoff, S.J., Ciciliano, J.C., Wells, M.N., Shah, A.M., Concannon, K.F., Donaldson, M.C., Sequist, L.V., Brachtel, E., Sgroi, D., Baselga, J., Ramaswamy, S., Toner, M., Haber, D.A., Maheswaran, S., 2013. Circulating breast tumor cells exhibit dynamic changes in epithelial and mesenchymal composition. Science 339, 580–584.